Eur Biophys J (1998) 27: 541–548

ARTICLE

S. Della Longa · M. Girasole · A. Congiu Castellano
A. Bianconi · A. P. Kovtun · A. V. Soldatov

Spin-resolved X-ray absorption near edge structure (XANES) simulation of metmyoglobin

Received: 8 October 1997 / Revised version: 10 March 1998 / Accepted: 23 March 1998

Abstract Spin resolved multiple scattering (MS) calculations of Fe K-edge X-ray Absorption Near Edge Structure (XANES) of myoglobin are reported for the first time. The observed differences of the Fe K-edge XANES spectra of sperm whale metmyoglobin under spin transition as a function of temperature have been studied. The method allows one to compute separately spin effects and local structural effects. The results show that spin effects are confined in the absorption rising edge in the range 7111–7130 eV, while purely structural effects are dominant in the range 7130–7170 eV. Symmetry changes of the Fe coordination sphere mainly related to its movement towards the heme plane, coupled to an increase of axial asymmetry, can explain the XANES changes observed above 7130 eV without an appreciable change of the Fe-N_p distance.

Key words Hemoproteins · Synchrotron radiation · Multiple scattering

Introduction

The spin state in hemoproteins is a characteristic feature of the Fe active site. In myoglobin it depends on many factors such as, for example, pH and ligand type. The study of the relationships between the Fe site structure and the Fe spin state is important because a spin transition can be accompanied by a change of the Fe ligand affinity and in turn of the biological functional state of the protein. Although many studies have addressed this subject no clear understanding of the correlation between the spin state and Fe-heme structure has been reached, the correlation being perhaps different for the various systems under study. The position of the iron atom in both high spin and low spin 6-coordinated ferric porphinato model systems is found within the heme plane, high spin model complexes having on average an expanded core size with respect to low spin model complexes (Scheidt and Reed 1981). On the other hand, an out-of-plane position of the iron atom, of about 0.4 Å, as in high spin 5-coordinated model complexes, is reported by diffraction data on sperm whale metmyoglobin (Takano et al. 1977). By contrast, in spite of similar pH and temperature conditions of the protein crystal, horse heart metmyoglobin has, according to X-ray data of Evans and Brayer (1990), a small Fe-heme displacement (0.03 Å, towards the water molecule). Moreover it is likely that very subtle local structural changes, difficult to detect by standard techniques, can affect the spin state, so that the spin/structure correlation remains an open question. Therefore developments of Fe-heme structure sensitive probes will be helpful to clarify the problem.

X-ray Absorption Near Edge Structure (XANES) spectroscopy is one such local probe (Pin et al. 1994). In this work we present an approach to the spin/structure problem in metmyoglobin, by analysing K-XANES spectra in the framework of the multiple scattering approach (MS), using spin resolved self consistent potentials. The K,L_1-edge XANES spectra measure dipole transition probabilities starting from the deep metal core level 1 s (or 2 s) ($\ell = 0$, $m_\ell = 0$) to delocalized final states with p-symmetry ($\ell = 1$, $m_\ell = 0, 1$). The XANES signal is due to positive interference between the outgoing photo-electron wave (produced by an absorption event) and the ingoing wave produced by multiple scattering of the same photoelectron from the surrounding atoms. So the energy position and intensity of a peak will depend on the geometry of the cluster of neighbouring atoms (bond distances and angles) and the actual potential seen by the photoelectron. In the common approach to XANES interpretation, the

S. Della Longa (✉)
Dipartimento Medicina Sperimentale, Università dell'Aquila,
Via Vetoio, Loc. Coppito II, I-67100 L'Aquila, Italy
e-mail: dellalonga@vaxaq.cc.univaq.it

M. Girasole · A. Congiu Castellano · A. Bianconi
Dipartimento Fisica, Università "La Sapienza" di Roma,
and INFM, Un. Roma,
I-00185 Roma, Italy

A. P. Kovtun · A. V. Soldatov
Department Solid State Physics, Rostov State University,
344104 Rostov-on-Don, Russia

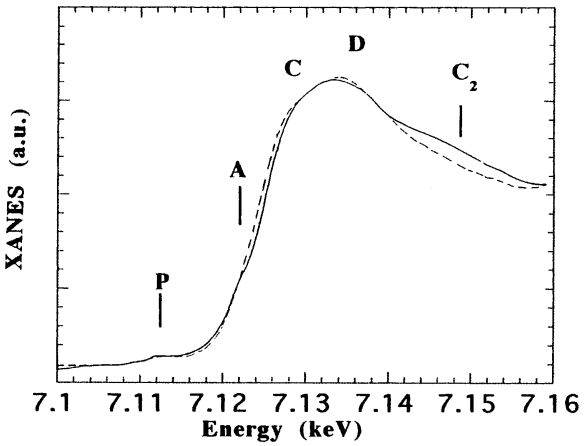

Fig. 1 Fe K-edge XANES spectra of high spin Fe(III) MbOH at pH = 10.5, T = 300 K (*dashed line*), and low spin Fe(III) MbOH at pH = 10.5, T = 80 K (*solid line*). Data taken from Oyanagi et al. (1987)

scattering of the photoelectron from electron charge distribution is considered to be dominant, whereas that from the spin of the valence electrons is neglected. Owing to the characteristic very fast coherence time (~10^{-15} s), the XANES signal probes the iron site conformations averaged over the protein ensemble, being close to that with highest probability.

Temperature dependent variations of the XANES of alkaline metmyoglobin from sperm whale, clearly related to the iron spin state, have been reported by Oyanagi et al. (1987) (Fig. 1). In fact, magnetic susceptivity data show that Fe(III) in this derivative is in a high spin state (S = 5/2) at room temperature, whereas at low temperature (80 K) it converts completely to a low spin state (S = 1/2). The XANES spectrum of metmyoglobin exhibits various features evolving with temperature: peak P is assigned to a dipole forbidden 1 s → 3 d electron transition, and contains contributions from both spin and structure. The other peaks A, C, D and C_2 have been interpreted in the case of deoxy-Mb (Bianconi et al. 1984), MbCO and MbCN (Bianconi et al. 1985a) as due to multiple scattering resonances, so they should depend on the overall geometry of the Fe site.

The first purpose of this study was to determine the Fe K-edge XANES sensitivity to iron spin state and related structural variations. We performed self-consistent spin resolved calculations of the electron structure of the Fe-heme complex. We used the resulting electron wave functions of high spin ($t_{2g}^3\ e_g^2$) and low spin (t_{2g}^5) Fe configurations in Fe(III)-myoglobin in order to simulate the K-XANES measured by Oyanagi et al. (1987). These calculations try to solve two Fe spin states, so they differ from the analogous calculations used by Soldatov et al. (1994) to simulate spin polarized Mn K-edge XANES of MnF_2 (in which transitions to final spin-up states and final spin-down states were separately measured, Hamalainen et al. (1992), as indicated in the method section.

The temperature dependent high spin → low spin transition in ferric metmyoglobin has been reproduced according to previous structural models. It is accompanied by a movement of the Fe atom toward the heme plane. This movement at low temperature is coupled with an increase of axial asymmetry (i.e., a decrease of the Fe-OH bond distance and an increase of the Fe-prox. His bond distance. The experimental XANES data are reproducible with very little variation of the Fe-N_p distance. According to our simulation, the low energy part of the spectrum is sensitive to both Fe spin state and Fe-heme structure.

Methods

XANES probes a scattering cluster (i.e. a group of atoms around an absorbing one) of a large size (Bianconi 1989). On the other hand it is time consuming to make self-consistent spin-dependent calculations within surch large clusters. Therefore, we divided our task into two parts: first we have obtained in a self-consistent mode two sets of spin-dependent molecular potentials, and second we have performed full multiple scattering calculations using a method appropriate for continuum states.

In order to obtain two sets of potentials for both high spin and low spin configurations we performed self-consistent spin-polarized calculations of the electronic structure of a small cluster: $FeON_5$ cluster that is a fragment of myoglobin. The method we used is based on the self consistent field scattered waves (SCF X_α-SW) technique with Slater X_α local density approximation (LDA) (Hohenberg and Kohn 1964), where a local exchange-correlation potential $V_{ex,\sigma}$ for electronic states with σ-type of spin can be written as

$$V_{ex,\sigma}(r) = -6\ \alpha\ [(3/4)\ \rho_\sigma(r)]^{1/3} \quad (1)$$

In this expression $\rho_\sigma(r)$ is the total local charge density of electrons with spin σ, and α is the exchange constant. Our approach is close to the standard technique of Johnson and Smith (1972). Its results are found to be in a good agreement with experimental data for heavy metal oxides, such as amorphous tantalum pentoxide (Gubskii et al. 1987) and uranium oxide (Garcia-Vidal et al. 1994).

In the high-spin (HS, S = 5/2) configuration, it is assumed that the five 3*d* electrons of the Fe^{3+} ion are "spin-up", while the 3*d* "spin-down" orbitals are unoccupied. In the low-spin (LS, S = 1/2) configuration, there are three spin-up electrons and two spin-down electrons. The exchange potential (1) for a given spin in our spin-polarized calculation is determined by the total electron distribution for that spin. When the number of spin-up and spin-down electrons are different (in the HS case the difference is equal to 5, while in the LS case it is equal to 1) the exchange potential tends to cause a splitting of the electronic structure of the cluster in the same manner as was found in early studies dealing with spin-polarized band structure calculations (Slater 1974). As a result one obtains spin-up and spin-down self-consistent potential functions for both the HS and LS configurations, i.e., four sets of embedded atomic potentials that we will refer as HU (high-up), HD

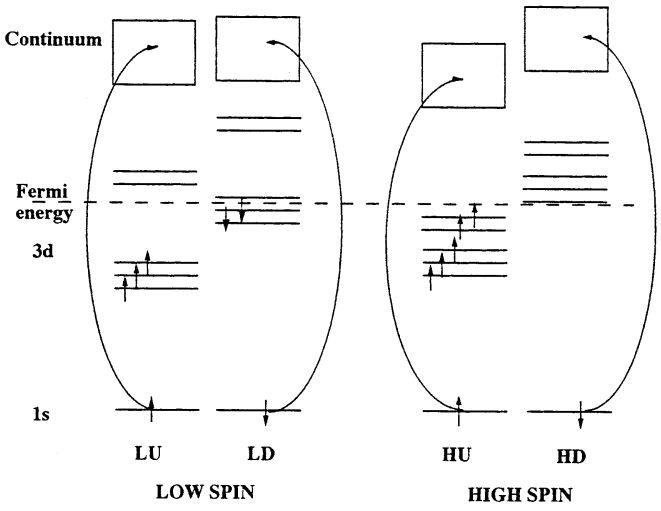

Fig. 2 Pictorial view of the processes considered in spin resolved XAS simulation. Different one-electron potentials and absorption probabilities are computed for each electron configuration (see the Method section)

(high-down), LU (low-up) and LD (low-down). A pictorial view of these four electron energy schemes is shown in Fig. 2.

We first considered the 1-shell $FeON_5$ cluster with C_{4v} symmetry around the central Fe atom. According to our procedure of muffin-tin potential construction (Della Longa et al. 1995) we obtained the following values of muffin-tin radii: 1.11 Å for central Fe, 0.896 Å for planar N, 0.988 Å for apical N and 0.859 Å for the O site sphere. We keep these values fixed going from the HS to the LS case, and during the iterative refinement, so that one can exclude artifactual charge transfers between muffin-tin spheres during the self consistency refinement procedure. The resulting averaged constant values of potential in the region between MT spheres (VMT) are –1.2018 Ryd, –1.2117 Ryd, –1.2265 Ryd and –1.2286 Ryd for the LU, LD, HU and HD potentials, the zero energy being chosen at the vacuum level. In the self-consistent procedure we have taken into account spherical harmonics with angular momentum ℓ = 0, 1 for oxygen and nitrogen spheres and ℓ = 0, 1, 2 for the iron sphere. The criterion of convergence of the self-consistency process was the inequality

$$\max |\rho_\sigma^{\ell+1}(r) - \rho_\sigma^{\ell}(r)| \leq 0.001 \qquad (2)$$

where i is the iteration number, $\rho(r)$ the electron charge density around each embedded atom, and σ the spin type. These potentials were used to calculate four sets of partial phase shifts of the photoelectron.

The XANES simulations make use of the one-electron full multiple scattering formalism (Durham et al. 1982), included in the G4XANES computer package developed by us (Della Longa et al. 1995). The calculations have been performed in real space for a three-shell cluster in the same manner as in our previous work (Bianconi et al. 1985a; Della Longa et al. 1993), where we did not consider the

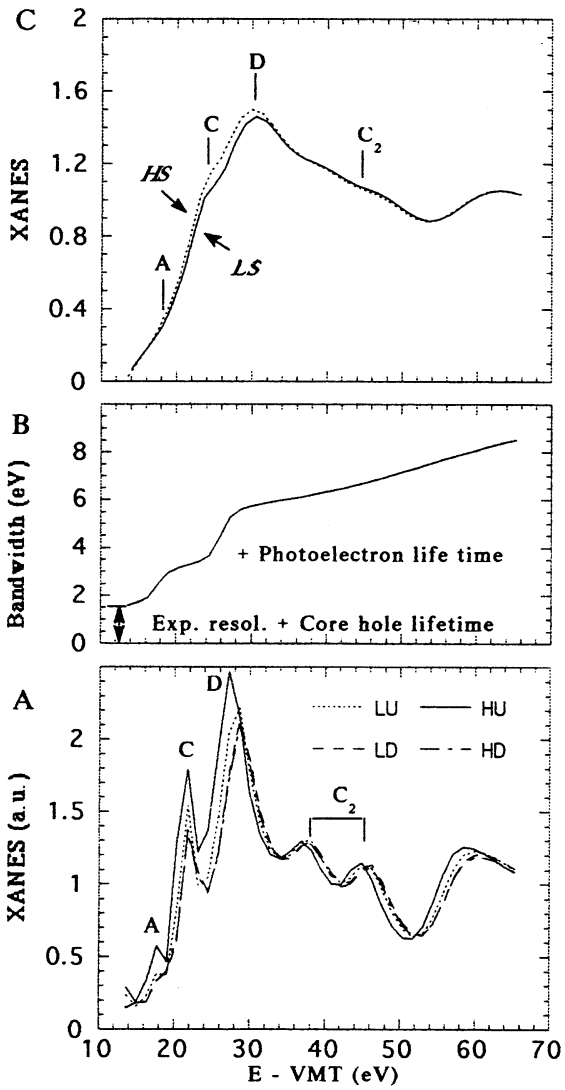

Fig. 3A–C Spin resolved XANES calculations related to a selected structural model: **A** Calculations for the four potential sets LU, LD, HU and HD. **B** Energy bandwidth function of final states in the Fe K-edge XANES due to core hole lifetime (1.2 eV), experimental resolution (0.5 eV) and photoelectron lifetime (energy dependent part). **C** Final simulation obtained by convoluting the energy bandwidth function with the calculated spectrum. Calculations considering high spin Fe (*solid curves*) and low spin Fe (*dashed curve*) are superimposed, allowing one to distinguish purely structural effects from spin effects. The zero energy is the averaged muffin-tin constant potential VMT

spin state. For each chosen structural model of the Fe-heme cluster four XANES spectra are calculated, corresponding to the HU, HD, LU and LD potential sets (Fig. 3A). The HU and LU spectra are always red-shifted by about 3 eV and 1 eV respectively from the analogous HD and LD spectra. The HS and LS XANES spectra are obtained simply as HS = (HU+HD)/2 and LS = (LU+LD)/2. A broadening Lorentzian function is applied to the calculated XANES to take into account the core hole lifetime (1.2 eV), the experimental resolution (0.5 eV) and an energy dependent factor representing the photoelectron lifetime

due to inelastic scattering by valence electrons (Fig. 3B). The energy dependent part is zero below the Fermi energy and contains jumps at the energies of plasmon excitations. Plasmon energies and jumps were chosen to be consistent with values found by electron energy loss experiments on Fe borides (Bratkovsky et al. 1994), then adjusted to fit the experimental data. These convoluted calculations (Fig. 3C) are then comparable with the experiment. The final difference in energy position of the absorption edge between HS and LS calculations is not greater than 0.5 eV.

The basic cluster used for the MS simulations has no symmetry, including 32 atoms from the porphyrin ring, the proximal histidine and the OH ligand. In spite of the great number of degrees of freedom, a large body of knowledge (essentially from crystallography and EXAFS) furnish ancillary information allowing one to select a limited number of parameters at the Fe-heme site in Mb, which are known to change dynamically and affect the XANES. The Fe-heme system has a pseudo-C_{4v} symmetry; the histidine ring and pyrrol rings of the porphyrin remain perfectly rigid. We have selected the following parameters: 1) d(Fe-N_p) (i.e. the equatorial first shell average distance from the pyrrol nitrogens in a C_{4v} symmetry); 2) and 3) d(Fe-N_ε) and d(Fe-O) (the axial distances of the proximal histidine and the OH ligand); 4) and 5) the rotation (tilting) angles of the same axial ligands; 6) the azimuthal angle of the proximal histidine; 7) the Fe displacement on the heme normal; 8) the heme "doming" (i.e., in-phase rotation of the four pyrrol rings, affecting in turn the equatorial first shell average distance); 9) the heme "ruffling" (i.e., opposite rotation of the two couples of opposite pyrrol rings, affecting the in-phase scattering of the equatorial ligands).

The fit goodness of the calculated vs. experimental data is reported below by using a fit index parameter F calculated as:

$$F = \sqrt{\chi^2} = \frac{1}{N\,\sigma^{exp}} \sqrt{\sum_i^N \left(y_i^{th} - y_i^{exp}\right)^2}$$

where N is the number of fitted points (N=40), σ^{exp} the experimental error (in the experiment of Oyanagi et al. (1987) a realistic value is $\sigma^{exp} = 2 \cdot 10^{-3}$ in normalized absorption units), y_i^{th} and y_i^{exp} the fitting and fitted absorption data, respectively. For known crystal structures, a good matching between calculations and experiments ifs found for the energy position of the peaks, while a poorer agreement on their intensity is expected.

The errors in applying XANES simulations to biological compounds, arise from different factors: i) The basic approximations in using the one-electron theory and the spherically averaged atomic potentials. ii) The high computational limits. The quantitative estimation of geometric parameters from XANES could be provided only by dynamical cluster simulations including all degrees of freedom. A first attempt to this challenging objective is in progress in our laboratory. iii) Different conformational substates at the metal site could exist (Parak et al. 1987; Hong et al. 1990). The XANES spectra in such a case probe the metal site structure averaged over the protein ensemble, being close to a particular conformation only if it has a high probability. The overall systematic errors are therefore in practice larger than those implicit in the relatively high sensitivity of XANES calculations in reproducing structural changes (e.g., bond lengths variations of 0.01 Å).

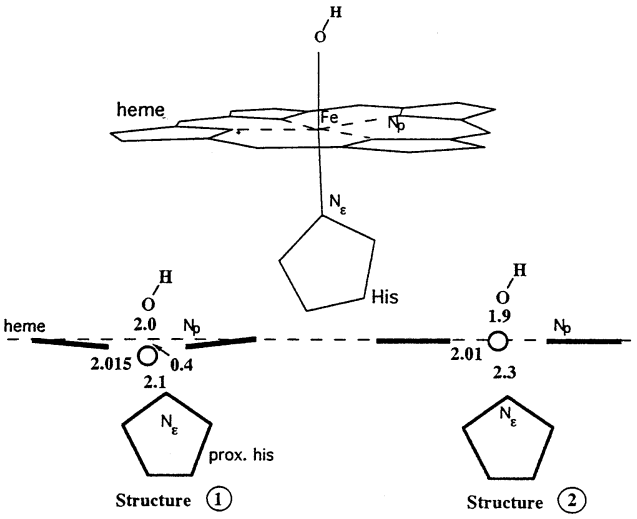

Fig. 4 Sketch of the heme-iron site in alkaline metmyoglobin. In the lower side, two examples of structural models, **1** (Fe out-of-plane) and **2** (Fe in-plane), used to model the spin/structure transition. The hydrogen atom of the OH^- ion is not considered in the calculations owing to its low scattering power

The structural models **1** and **2** giving the best fit of the calculated vs. experimental data (see the Results section) are reported in Fig. 4. We note that the calculated total energies of clusters **1** in the two spin states of Fe were $E_{tot}^{LS} = -3338.56$ Ryd, and $E_{tot}^{HS} = -3338.67$ Ryd, with a difference of $\Delta E_{tot}^{HS-LS} = -0.11$ Ryd, still too large to explain spin equilibrium in metmyoglobin (thermodynamic energy difference between spin states according to a Boltzmann distribution model: $\Delta G \approx 1$ kJ/M = $7 \cdot 10^{-4}$ Ryd (Beetlestone and George 1964); estimated proximal work necessary to move the iron atom onto the heme plane in a newtonian elastic approximation: $\Delta H \approx 3 \cdot 10^{-3}$ Ryd (Champion 1989). This gives an idea of the roughness of the (SCF X_α-SW) approximation usually applied in biological contexts.

Results

As described in the method section, owing to computational limits we calculated the XANES for a limited number of conformations, varying all of the nine parameters affecting the Fe-heme dynamics. The XANES fit was found to be very sensitive, in decreasing order, to: first shell distances (parameters 1, 2 and 3 mentioned in the method section), the iron displacement (parameter 7), the tilting angle of the axial parameter (parameters 4 and 5) the heme doming and ruffling (parameters 8 and 9) and the azimuthal histidine angle (parameter 6).

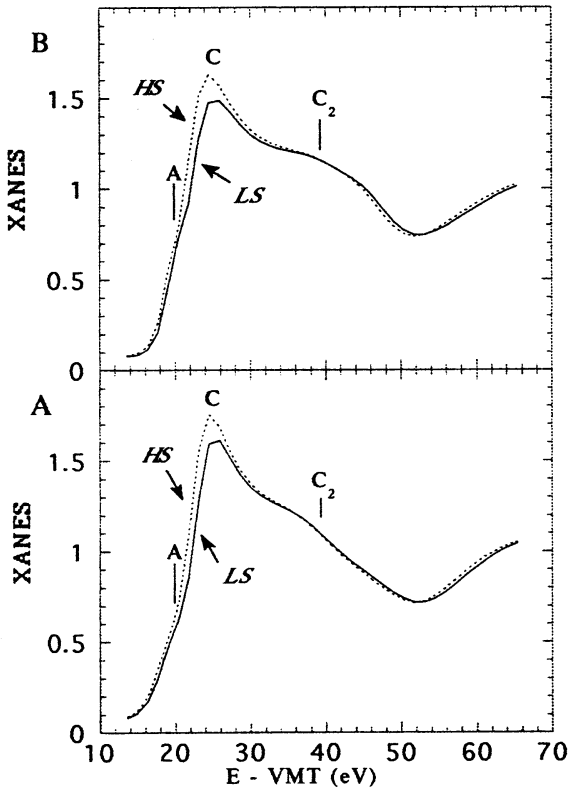

Fig. 5 Spin resolved 1-shell XANES calculations related to **A** Fe out-of-plane, lower axial asymmetry, and **B** Fe in-plane, higher axial asymmetry. Calculations considering high spin Fe (*dotted curves*) and low spin Fe (*solid curves*) are superimposed, allowing one to distinguish purely structural effects from spin effects

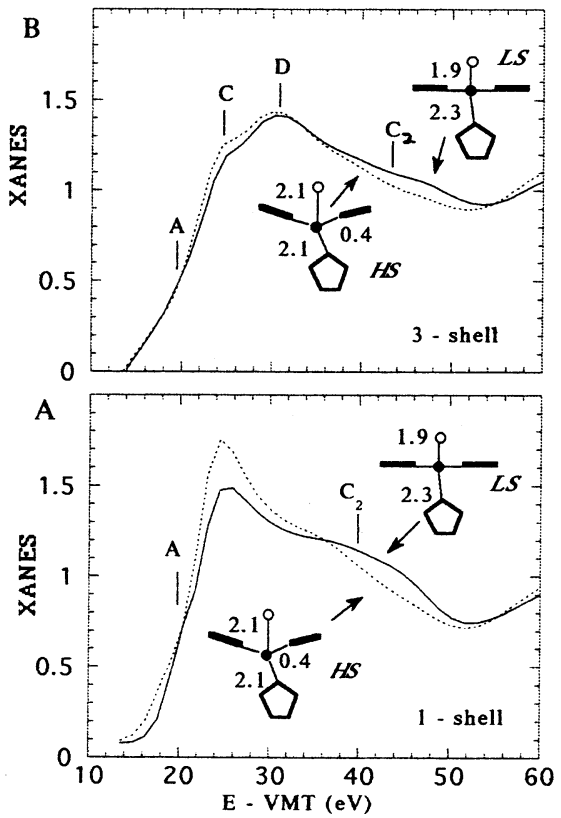

Fig. 6A, B Simulation of the XANES experiment reported in Fig. 1, giving best fit among the selected structural models. **A** 1-shell calculations. **B** 3-shell calculations. The fit goodness to the experimental spectra of HS and LS $Mb^{+}OH^{-}$ is F = 2.96 and F = 3.2, respectively

Two structural models, giving the best fit to the experimental XANES spectra, are considered in more detail in the present work (Fig. 4). In structure **1**, the Fe is 0.4 Å out of the N_p plane, with the hydroxyl oxygen at 2.0 Å and the imidazole nitrogen at 2.1 Å. In the structure **2**, the Fe is in the N_p plane, with the hydroxyl oxygen at 1.9 Å and the imidazole nitrogen at 2.3 Å. The Fe-N_p distance is constrained between 2.01 Å (structure **2**) and 2.015 Å (structure **1**) by doming the heme.

To solve spin and structural effects, we have applied both the high spin and low spin potential to each of the structural models. The theoretical XANES for structure **1** with high spin Fe (solid curve) and low spin Fe (dashed curve) are shown in Fig. 5A. The theoretical XANES for structure **2** with high spin and low spin Fe are shown in Fig. 5B. Every time the calculation has been carried out for a certain structural model, spin effects have proven negligible 30 eV beyond the intersphere potential of the muffin-tin approximation. On the other hand, symmetry changes of the Fe coordination sphere determine marked XANES changes in the 30–50 eV energy region. Spin effects influence to some extent the absorption edge: the ideal, simple high spin → low spin rearrangement of the d-electrons (computed without structural changes) produces a blue-shift of the absorption edge of about 0.5–1.0 eV and a small decrease of the main absorption peak in the case of both structures **1** and **2**. This spin dichroism is explained theoretically by a spin sensitivity of both the dipole transition matrix elements (that influence the relative intensity of XANES) and atomic scattering phase shifts that influence the energy position of the absorption edge and of the peaks (Soldatov et al. 1995).

The 1-shell calculations do not satisfactorily reproduce the experimental spectrum of metmyoglobin. For example peak D observed in the experiment (Fig. 1) is not reproduced in the calculations; this peak has been assigned to multiple scattering involving the 2nd and the 3rd shell of the porphyrin plane (see below). Apart from peak D, however, the observed experimental trend can be reproduced by a movement of the iron atom towards the heme plane (with changes in the Fe-N_p distance less than 0.005 Å). The energy positions of peak A and peak C in the 1-shell simulation are related to the Fe-His distance and the Fe-N_p distance respectively; they are weakly resolved in cluster **1**, for which d(Fe-N_p)-d(Fe-His) = 0.1 Å but become well resolved (and peak A becomes evident) in cluster **2**, for which d(Fe-N_p)-d(Fe-His) = 0.4 Å. The intensity of peak C_2 is mainly related to the Fe-C_t distance, becoming prominent when the iron lies in the heme plane. The ability to reproduce the trend at peaks A and C_2 by 1-shell calculations is a direct indication that

the Fe coordination symmetry transforms in the experiment[1].

The experiment of Oyanagi reported in Fig. 1 is theoretically reproduced in Fig. 6. The 1-shell calculations for cluster **1** (Fe out-of-plane) using high spin potentials (plotted curve), and for cluster **2** (Fe in-plane) using low spin potentials (solid curve) are reported in Fig. 6A. The 3-shell calculations of the same spectra are reported in Fig. 6B. It is clear that to reproduce all the experimental features it is necessary to consider a 3-shell scattering cluster containing the complete porphyrin macrocycle and the proximal histidine. The 3-shell XANES simulation reproduces the experimental trend concerning all the features A, C, D and C_2, with a fit goodness F = 2.96 for the HS case, and F = 3.2 for the LS case. The feature C_2 receives pure structural contributions, being more pronounced when the iron lies in the N_p plane, with a marked axial asymmetry. On the other hand the rising energy region depends on both spin state and structure (as seen above), or, in other words, structural effects are unresolvable from spin effects below 7130 eV. To interpret peak A is further complicated because partial charge transfers from (to) the iron atom induce shifts of the absorption edge.

Other structural models that can be chosen to simulate the HS → LS transition of Mb^+OH^- are shown in Fig. 7, frames A, B and C. Dotted curves correspond to simulations performed with HS potentials, while solid lines correspond to simulations performed with LS potentials. The effect of axial asymmetry changes, with the Fe atom restrained in the heme plane, is reported in Fig. 7A. The calculated fit goodness is F = 4.38 for the HS state, and F = 3.2 for the LS state. The same effect of axial asymmetry changes, with the Fe atom restrained out of the heme plane, is reported in Fig. 7B, giving F = 4.03 for the HS state, and F = 4.11 for the LS state. The effect of in-plane movement of the Fe atom, within the same axial asymmetry, is shown in Fig. 7C, giving F = 3.91 for the HS state, and F = 5.71 for the LS state.

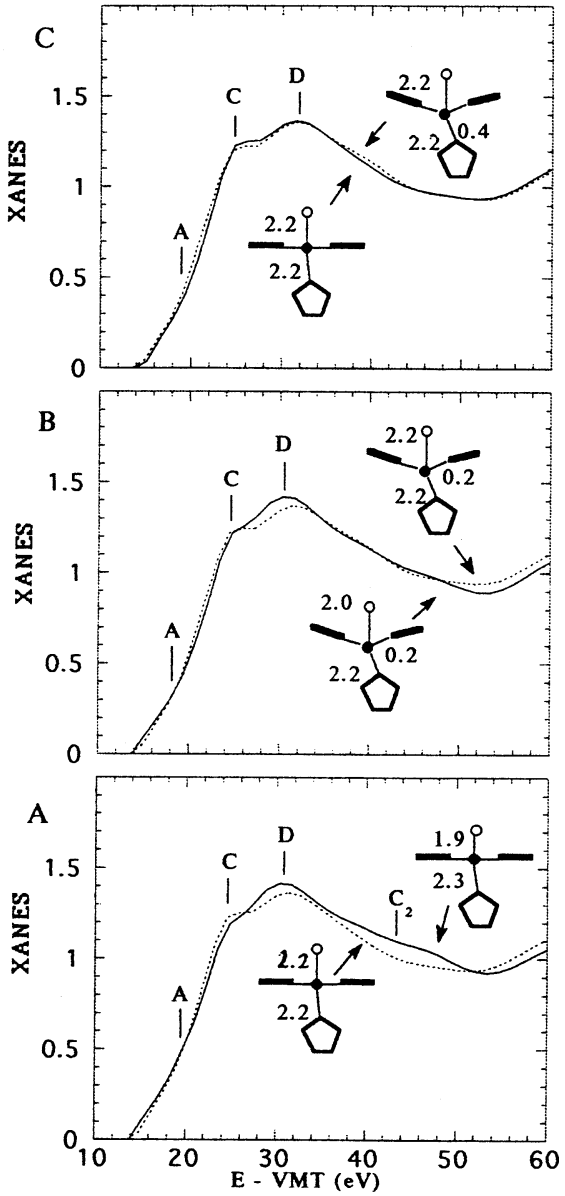

Fig. 7A–C Other structural simulations of the XANES experiment on HS → LS transition of Mb^+OH^-. *Dotted curves* correspond to simulations performed with HS potentials, *solid lines* correspond to simulations performed with LS potentials. **A** axial asymmetry changes, with the Fe atom restrained in the heme plane; **B** axial asymmetry changes, with the Fe atom restrained out of the heme plane; **C** in-plane movement of the Fe atom, within the same axial asymmetry

Discussion

Our method allows one to calculate separately the contribution of spin effects and structural effects in the XANES spectrum of myoglobin: as pointed out in the Result section, according to our simulations one expects these effects to be experimentally unresolvable in the energy range below 7130. In contrast, purely structural effects are predicted beyond 7130 eV. Even if XANES cannot be considered as a fully exact method to quantitatively measure structural parameters (in fact in the calculations the differences between features A and C_2 are somewhat smaller than in the experiment) the calculations make it possible to interpret the origin of spectral changes in structural terms. The XANES spectra measured by Oyanagi et al. (1987) are explained according to a model relating the Fe

[1] Our spin resolved 1-shell calculations are predictive of XANES changes observed in spin transitions of non-heme proteins containing 6-coordinated iron. It is the case in HS Fe(II) bleomycin and LS Fe(III) bleomycin (reported by Westre et al. (1995)). The large shift of the absorption edge is easily explained by summing up spin effect, increasing of Fe charge, and decreasing of the Fe-N_p distance (reported by authors by EXAFS analysis). Moreover the XANES difference in shape (neglected by the authors), according to our 1-shell calculations can be attributed to displacement of the iron from the equatorial plane of the octahedral coordination. Peroxo Fe(III) LS bleomycin has 6-coordinated iron in the equatorial plane with small distortions from full octahedral geometry, while in HS Fe(II) bleomycin Fe is out of the equatorial plane, with a large distortion from octahedral symmetry

spin state to the Fe position with respect to the heme plane. In sperm whale high spin metMb the Fe atom is out-of-plane by at least 0.3 Å, as reported by Takano et al. (1977). The temperature dependent high spin → low spin transition is accompanied by a movement of the iron atom towards the heme plane. This movement should increase the Fe- prox. His distance, changing in turn the axial asymmetry at the Fe site. The axial asymmetry is thought to be a consequence of the electronegativity difference between the imino nitrogen from proximal histidine and the hydroxyl oxygen. We note here that most of the data on high spin 6-coordinated porphinato models, reporting in-plane Fe, refer to complexes with the same ligand type in the 5th and 6th position of the Fe coordination, so simply by symmetry arguments the iron must be in-plane without any axial asymmetry. According to extensive MS calculations (not shown here), even by considering other degrees of freedom (heme core size expansion or heme ruffling) it is not possible to fit the trend of peak C_2 without considering the iron displacement.

The experimental absorption edge (Fig. 1) shifts very little (about 0.5 eV after peak A, as predicted by theory for spin effects). The absorption edge has been reported to shift depending also on Fe-N_p distance and Fe net charge. By assuming that these two parameters remain nearly constant during the spin transition (having restrained the Fe-N_p distance between 2.01 and 2.015 Å) the theoretical spectra aligned in energy to the experimental ones. It is not possible by XANES to solve ambiguities about the mechanisms involved in the absorption edge shifts, however changes in the Fe-N_p distance could be easily probed by EXAFS (Eisenberger et al. 1978).

Concerning previous MS simulations, two points have to be clarified:

i) Oyanagi et al. (1987) observed that previous calculations applied to the Fe-heme displacement in deoxy-Mb did not reproduce the changes in regions A and C_2 as a consequence of the out-of-plane movement of the iron atom. However, on the basis of the MS theory, it is not possible to compare the previous calculations on 5-coordinated Fe with those on 6-coordinated iron with pseudo octahedral symmetry.

ii) It is useful to compare the XANES simulation on MbCO (Bianconi et al. 1985a, discussed in the paper of Oyanagi et al. (1987)) with the present one on MbOH. In the case of MbCO, it was shown that peaks C_1 and C_2 are strongly polarized along the heme axis according to experimental polarized XANES. The peaks were fully reproduced by MS calculations and explained as being due to a focusing effect (i.e., in-phase electron back-scattering from the C and O atoms of the bonded CO molecule, the bending angle Fe-C-O being about 150 degrees). According to MS calculations of the same work, when the ligand bending angle increases, the focusing effect (and the C1 and C2 resonances due to the ligand) decreases, and peak A at about 10 eV appears (curve d of Fig. 2 in the paper of Bianconi et al. (1985a). This last theoretical curve exhibits all the features of the simulated low spin MbOH of the present work: so it is expected that the scattering properties of a diatomic ligand with large bending angle are intermediate between that of a diatomic ligand with efficient focusing effect (oriented upright), and that of a monoatomic ligand such as OH, or OH_2 (hydrogen atoms show negligible electron scattering).

It is noticeable that in the paper of Oyanagi et al. (1987) there is great similarity between the experimental spectra of MbO_2 and low spin $MbOH^-$, that confirms this assumption. This similarity can be explained only by i) a close structural analogy between the Fe site in Fe(II) MbO_2 and that in Fe(III) $MbOH^-$; and ii) similar electron scattering properties of the axial ligands O_2 and OH, due to the large bending angle of O_2 (Fe-O-O of about 120°). In sperm whale MbO_2 d(Fe-O) = 1.83 Å, d(Fe-N_ε) = 2.07 Å, d(Fe-N_p) = 1.96 Å, and the Fe lies in the heme plane, with an overall structure close to that used by us in cluster **2**.

In spite of the fact that, owing to the physical origin of the signal (electron multiple scattering), the Fe displacement coupled to asymmetry changes are certainly not the only parameters that can theoretically affect the C_2 feature, the XANES calculation fits made on the overall spectra suggest that these parameters are involved in the spin transition of Mb, affecting the C_2 feature. On the basis of these calculations, the feature C_2 could be assumed experimentally, rather than a spin-state marker, as a direct spectroscopic probe of the structural state of the Fe-heme system along a generalized coordinate Q that links the in-plane movement of the iron to the readjustment of its coordination sphere. Now the question that arises is whether it is possible to find a more general correlation between this spectroscopic probe, the spin state, and the Fe-heme local structure, at least within a limited group of hemoproteins. Such a correlation would open up the possibility to directly study, by XANES, intermediate configurations of the Fe-heme moiety between the so far discussed high affinity and low affinity forms of ligated myoglobin.

The feature C_2 is prominent in O_2 ligated and CO ligated hemoproteins for which the Fe^{2+} ion has been reported in plane. Pure REDOX changes, such as spin changes, should not affect the C_2 feature: they should result in a rigid shift of the XANES spectrum without important changes in shape (it is the case of cytochrome C, or the transient intermediate in the reaction of cyanide metmyoglobin with dithionite, Saigo et al. (1993); therefore it is a reasonable assumption that the feature C_2 probes the Q coordinate in the case of hemoproteins with monoatomic ligands such as Mb^+OH^-, Mb^+OH_2 or diatomic ligands with large bending angle, such as MbO_2, MbNO, and maybe Mb^+N_3. More caution is necessary when considering that an efficient focusing effect from the sixth ligand (as in MbCO, Mb^+CN and imidazole Mb^+) can modulate the feature C_2. Other interesting cases such as sulfur-ligated and fluorine-ligated hemoprotein are out of the scope of this study because of the different scattering properties of these ligands.

Finally, we note that sometimes the spin/structure correlation is certainly different, as in the relevant case of carp azidomethemoglobin (Perutz et al. 1978; Noble et al. 1983). It has been reported that this hemoglobin in the pres-

ence of inositol hexaphosphate (IHP) is in a pH dependent equilibrium between low affinity and high affinity quaternary structures. Two spin states of Fe-heme are related to these low affinity and high affinity forms, the effective magnetic moment changing from 2.83 μ_B (pH > 6.5) to 4.2 μ_B (pH < 6.5), the high spin form having higher affinity for azide. Their reported XANES spectra (Bianconi et al. 1985b) change very little under spin conversion, and peak C_2 slightly increases in parallel with the high spin percentage, unlike with metmyoglobin. This finding is consistent with the present study, by assuming a different mechanism to account for the (small) average structural rearrangement of the Fe-hemes under spin transition, including rotation of the azide bending angle, and rotation of the proximal histidine tilting angle, with a constrained movement of the Fe atom towards the heme plane in the high spin form with higher affinity.

Acknowledgements This work was supported by Grant of CNR (Biotechnologies), Italy, by INTAS-94-3899 program, and NATO Linkage Grant CRG 930305.

References

Beetlestone J, George P (1964) A magnetical study of equilibria between high and low spin states of metmyoglobin complexes. Biochemistry 3: 707–714

Bianconi A, Congiu Castellano A, Dell'Ariccia M, Durham PJ, Burattini E, Barteri M (1984) XANES study of iron displacement in the haem of myoglobin. FEBS Letters 178: 165–170

Bianconi A, Congiu Castellano A, Durham PJ, Hasnain SS, Phillips S (1985a) The CO bond angle of carboxymyoglobin determined by angular-resolved XANES spectroscopy. Nature 318: 685–687

Bianconi A, Congiu Castellano A, Dell'Ariccia M, Giovannelli A, Morante S (1985b) Constraints of T conformation of carp azide hemoglobin on Fe site structure. FEBS Letters 191: 241–244

Bianconi A (1989) XANES spectroscopy. In: Prinz R, Koningsberger D (eds) X ray absorption: principles, applications and techniques of EXAFS, SEXAFS and XANES. Wiley, New York, pp 573–653

Bratkovsky AM, Rashkeev SN, Smirnov AV, Wendin G (1994) Universality in electronic structure and EELS spectra of FeB and NiB crystalline and amorphous systems. Europhys Lett 26: 43–49

Champion PM (1989) Resonance Raman and site-directed mutagenesis studies of myoglobin dynamics. In: Jardetzky O (ed) Protein structure and engineering. Plenum Press, New York, pp 347–354

Della Longa S, Bianconi A, Palladino L, Simonelli B, Congiu Castellano A, Borghi E, Barteri M, Beltramini M, Rocco GP, Salvato B, Bubacco L, Magliozzo RS, Peisach J (1993) A XANES study of metal coordination in Co(II)-substituted Carcinus maenas hemocyanin. Biophys J 65: 2680–2691

Della Longa S, Soldatov A, Pompa M, Bianconi A (1995) Atomic and electronic structure probed by X-ray absorption spectroscopy: full multiple scattering analysis with the G4XANES package. Computational Mat Sci 4: 199–210

Durham P, Pendry JB, Hodges CH (1982) Calculation of X-ray absorption near edge structure, XANES. Comput Phys Commun 25: 193–200

Eisenberger P, Shulman RG, Kincaid BM, Brown GS, Ogawa S (1978) Extended X-ray absorption fine structure determination of iron nitrogen distances in haemoglobin. Nature 274: 30–34

Evans SV, Brayer GD (1990) High resolution study of the three dimensional structure of horse heart metmyoglobin. J Mol Biol 213: 885–897

Garcia-Vidal FJ, Merino J, Perez R, Rincon R, Ortega J, Flores F (1994) Density-functional approach to LCAO methods. Phys Rev B 50: 10537–10547

Gubskii AL, Kovtun AP, Khanin SD (1987) Cluster modeling of the electron structure in amorphous tantalum pentoxide. Sov Phys Solid State 29: 611–616

Hamalainen K, Kao CC, Hastings JB, Siddons DP, Berman LE, Stojanoff V, Cramer SP (1992) Spin dependent x-ray absorption of MnO and MnF_2. Phys Rev B46: 14274–14277

Hohenberg P, Kohn W (1964) Inhomogeneous electron gas. Phys Rev 136: 864–871

Hong MK, Braunstein D, Cowen BR, Frauenfelder H, Iben IET, Mourant JR, Ormos P, Scholl R, Schulte A, Steinbach PJ, Xie A, Young RD (1990) Conformational substates and motions in myoglobin. Biophys J 58: 429–436

Johnson H, Smith FC (1972) Chemical bonding of a molecular transition-metal ion in a crystalline environment. Phys Rev B5: 831–843

Noble RW, De Young A, Di Iorio EE, Winterhalter KH, Cerdonio M, Morante S, Vitale S (1983) Quaternary structure and spin equilibria in ferric hemoglobins. A room temperature study. Eur J Biochem 133: 475–478

Oyanagi H, Iizuka T, Matsushita T, Saigo S, Makino R, Ishimura Y, Ishiguro T (1987) Local structure of heme-iron studied by high-resolution XANES; thermal spin equilibrium in myoglobin. J Phys Soc Jpn 56: 3381–3388

Parak F, Hartmann H, Aumann KD, Reuscher H, Rennekamp G, Bartunik H, Steigemann W (1987) Low temperature X-ray investigation of structural distributions in myoglobin. Eur Biophys J 15: 237–249

Perutz MF, Sanders JKM, Chenery DH, Noble RW, Pennelly RR, Fung LWM, Ho C, Giannini I, Porschke D, Winkler H (1978) Interactions between the quaternary structure of the globin and thespin state of the heme in ferric mixed spin derivatives of hemoglobin. Biochemistry 17: 3640–3651

Pin S, Alpert B, Congiu Castellano A, Della Longa S, Bianconi A (1994) X-ray absorption spectroscopy of hemoglobin. Methods Enzymol 232: 266–292

Saigo S, Hashimoto H, Shibayama N, Nomura M, Nagamura T (1993) X-ray absorption spectroscopic study of a transient intermediate in the reaction of cyanide metmyoglobin with dithionite by using rapid freezing. Biochim Biophys Acta 1202: 99–106

Scheidt WR, Reed CA (1981) Spin-state/stereochemical relationships in iron porphyrins: implications for the hemoproteins. Chem Rev 81: 543–555

Slater JC (1974) Self consistent field for molecules and solids. McGraw-Hill, New York

Soldatov AV, Ivanchenko TS, Kovtun AP, Della Longa S, Bianconi A (1995) Spin-dependent Mn K-edge XANES of MnO and MnF_2: full multiple scattering analysis. Phys Rev B52: 11757–11762

Takano T (1977) Structure of myoglobin refined at 2.0 A resolution. J Mol Biol 110: 537–568

Westre TE, Loeb KE, Zaleski JM, Hedman B, Hodgson KO, Solomon EI (1995) Determination of the geometric and electronic structure of activated bleomycin using X-ray absorption spectroscopy. J Am Chem Soc 117: 1309–1313